JOURNAL OF VIROLOGY, Sept. 2002, p. 9537–9544 Vol. 76, No. 18
0022-538X/02/$04.00+0 DOI: 10.1128/JVI.76.18.9537–9544.2002

Growth of Rotaviruses in Primary Pancreatic Cells

Barbara S. Coulson,[1]* Paul D. Witterick,[1,2] Yan Tan,[1] Marilyn J. Hewish,[1] Joanne N. Mountford,[2] Leonard C. Harrison,[2] and Margo C. Honeyman[2]

Department of Microbiology and Immunology, The University of Melbourne, Royal Parade, Victoria 3010,[1] and Autoimmunity and Transplantation Division, Walter and Eliza Hall Institute of Medical Research, Melbourne, Victoria 3050,[2] Australia

Received 26 November 2001/Accepted 12 June 2002

Rotavirus infection in children at risk of developing type 1 diabetes has been temporally associated with development of pancreatic islet autoantibodies. In this study, nonobese diabetic mice were shown to be susceptible to rhesus rotavirus infection and pancreatic islets from nonobese diabetic mice, nonobese diabetes-resistant mice, fetal pigs, and macaque monkeys supported various degrees of rotavirus growth. Human rotaviruses replicated in monkey islets only. This islet susceptibility shows that rotavirus infection of the pancreas in vivo might be possible.

Rotaviruses are the major cause of human infantile gastroenteritis worldwide, with multiple serotypes causing regular winter outbreaks until herd immunity is almost complete by 5 years of age (4). These nonenveloped, triple-layered, double-stranded RNA viruses are members of the family *Reoviridae* (13). Their outer capsid is composed of the glycoprotein VP7, through which spikes of the protein VP4 protrude (45). Both VP4 and VP7 independently elicit neutralizing, protective antibodies and are serotype determinants (40). VP4 is an important determinant of virulence, host cell tropism (28), receptor binding, and cell penetration (31, 35). Proteolytic cleavage by pancreatic trypsin of VP4 into two subunits, VP8* and VP5*, is required for virus infectivity and promotes rapid virus internalization into the cell. VP6 forms the capsid underlying the outer capsid and determines group and subgroup specificity (13).

Rotaviruses normally infect the mature enterocytes of the small intestine but may spread extraintestinally. Indications of rotavirus infection of the liver in humans include elevated liver aminotransferase activity during rotavirus infection (17), rotavirus particles in a liver abscess (18), and rotavirus replication in HepG2 cells (32, 52). In children with severe combined immunodeficiency (SCID) and chronic rotavirus infection, replicating rotavirus is present in the liver and kidneys and rotavirus antigen is detectable in the serum (16, 51).

Severe rotavirus gastroenteritis has been associated with pancreatitis in two children (12, 39) and with nonketotic hyperglycemic syndrome in one child (48). Extraintestinal rotavirus detection in these children was not attempted. Pancreatic islet cell autoantibodies were detected in acute-phase but not convalescent-phase serum from one child (39). These antibodies are markers of islet autoimmunity and predict the T-cell-mediated destruction of islet β cells, leading to type 1 diabetes (T1D). In addition to islet cell autoantibodies, the subclinical autoimmune prodrome of T1D is characterized by circulating autoantibodies to insulin, glutamic acid decarboxylase (GAD), and tyrosine phosphatase-like islet antigen 2 (IA-2) (20). We detected autoantibodies to GAD and to IA-2 in acute- and/or convalescent-phase sera of 3 (30%) of 10 children without a family history of diabetes who were hospitalized with rotavirus gastroenteritis (24). This rate was at least four times that observed in normal schoolchildren (2).

The strong environmental influence on the development of T1D (21) has led to numerous studies of potential viral trigger agents in humans and in murine models (29, 49). We recently reported evidence of a link between rotavirus infection and T1D in humans genetically at risk for this disease (25, 26). The immunodominant T-cell epitope of the islet antigen IA-2, amino acids (aa) 805 to 820, was found to have 33 to 56% identity and 100% similarity over 9 aa (aa 41 to 49) of rotaviruses of VP7 serotypes 1 and 3 (26). The T-cell contact residues in the IA-2 and VP7 sequences appeared to be identical, indicating a potential for molecular mimicry. Only 11 aa N terminal of this VP7 sequence is a 12-aa sequence at positions 18 to 30 that shows 67% identity and 92% similarity to aa 117 to 128 of GAD. All human rotaviruses contain the GAD-related sequence. This GAD sequence encompasses a T-cell epitope in DR4 transgenic mice and in DR4-DQ8 homozygous at-risk humans. Both the GAD- and IA-2-related sequences in VP7 contain hydrophobic potential anchor sequences for binding to HLA class II molecules and are flanked by epitopes for anti-rotavirus $CD8^+$ cytotoxic T cells in C57BL/6 and BALB/c mice (5, 15), confirming that this VP7 region is strongly immunogenic.

Evidence suggestive of a clinical association between rotavirus infection and T1D was obtained from 54 children at risk for T1D in whom rotavirus seroconversion in immunoglobulin A (IgA) or IgG was significantly associated in the same 6-month period with the first appearance of, or a significant increase in, IA-2 antibodies, GAD antibodies, and/or antibodies to insulin (25). There was no cross-reaction between anti-rotavirus and anti-islet antibody responses, as absorption of sera with viral antigen did not affect anti-islet antibody levels (25). Rotavirus infection may trigger islet autoimmunity and

* Corresponding author. Mailing address: Department of Microbiology and Immunology, The University of Melbourne, Royal Parade, Victoria 3010, Australia. Phone: 61 3 8344 8823. Fax: 61 3 9347 1540. E-mail: barbarac@unimelb.edu.au.

hasten the onset of clinical diabetes in genetically at-risk children.

Direct pancreatic involvement during experimental rotavirus infection was examined by using porcine rotavirus strain OSU, which was not detected in piglet pancreata (54). Porcine islets are surrogates for human islets (47) and are being evaluated as xenografts (33). No studies of pancreatic involvement during rotavirus infection of monkeys or mice have been reported. In monkeys, simian rotavirus strain SA11 produced enteric infection, diarrhea, or generalized infection and diarrhea, depending on the species (53). Rhesus rotavirus (RRV) induced hepatitis in 21% of normal mice and 84% of neonatal SCID mice, and strain SA11 induced mild hepatitis in SCID mice (57), demonstrating extraintestinal spread. It has been proposed that RRV induces extrahepatic biliary atresia in newborn BALB/c mice (44). Reovirus, also a member of the *Reoviridae* family, has long been implicated in extrahepatic biliary atresia in mice (56). Mammalian reoviruses infect murine pancreatic β cells to produce a T1D-like syndrome (22, 41) that can be associated with autoantibodies to insulin (42). Reovirus infection of human islets results in increased MHC class I protein expression and β-cell death (7, 56).

The nonobese diabetic (NOD) mouse is the favored animal model for human T1D. Its MHC class II (I-A^{g7}) is structurally and functionally similar to HLA-DQ8 (*0302), the major susceptibility class II molecule in humans, and it displays immunity to the same islet antigens as that of humans (1). Spontaneous destruction of β cells occurs in response to macrophage and lymphocyte infiltration of the islets (insulitis), beginning at 3 to 4 weeks of age. Most mice succumb to diabetes by 16 to 20 weeks. Coxsackievirus B4 infection of NOD mice produces severe pancreatitis starting at 3 days postinfection (p.i.) (27). In contrast, the nonobese, diabetes-resistant (NOR) mouse that has 88% of the NOD genome, including the diabetogenic MHC (46), exhibits protracted, nondestructive peri-insulitis (14). No studies of rotavirus infection of NOD or NOR mice have been reported.

In this study, we examined the ability of RRV to infect NOD mice and tested islets and islet cell-depleted pancreatic cells from NOD and NOR mice, fetal porcine islets, and monkey islets for susceptibility to infection with human and monkey rotaviruses.

RRV infects NOD mice. The viruses used in this study, monkey rotaviruses RRV and SA11, of serotypes P5B[3], G3 and P5B[2], G3, respectively, and human rotavirus strains Wa (P1A[8], G1), RV-5 (P1B[4], G2), and P (P1A[8], G3), have been described previously (8). Virus infectivity was activated by treatment with porcine pancreatic trypsin type IX (10 μg/ml; Sigma Chemical Co., St. Louis, Mo.) for 20 min at 37°C. Viruses were propagated in confluent MA104 cells in Dulbecco's modified Eagle's medium (DMEM) containing porcine trypsin at 1 μg/ml (DMEM-T) as previously described (23, 50). Control, uninfected MA104 cell lysate was prepared by mock infection of MA104 cells with DMEM containing porcine trypsin at 10 μg/ml. After incubation at 37°C for 2 to 5 days, virus-infected and mock-infected cells were lysed by three rounds of freeze-thawing at −70°C and harvested cells were clarified by centrifugation at 1,500 × *g* for 7 min. Uninfected MA104 cell lysate was treated with trypsin at 10 μg/ml for 20 min at 37°C before use. The identities of the rotaviruses used were confirmed by RNA gel electrophoresis (8).

NOD mice (NOD/Jax) and diabetes-resistant NOR mice (NOR/Lt), obtained from the Jackson Laboratory (Bar Harbor, Maine), were maintained at the animal facilities of the Walter and Eliza Hall Institute and the Department of Microbiology and Immunology of The University of Melbourne under specific-pathogen-free conditions and housed in microisolator cages. All procedures were conducted in accordance with protocols approved by the Walter and Eliza Hall Institute Animal Ethics Committee or the Animal Experimentation Ethics Sub-Committee of The University of Melbourne, as appropriate. Both NOD and NOR mice are H-2 K^d D^b I-A^{g7}, I-E negative. Female and male NOD mice in these facilities have diabetes incidences of ≥70% and ≤45%, respectively, by 250 days of age. The sera collected from the 100 NOD and NOR mice used in our experiments all showed negative anti-rotavirus antibody titers of <1:50 by an enzyme immunoassay (EIA) which was done as previously described (10) with partially purified RRV as the capture antigen. The viral antigens reactive in this assay are VP6, VP4, and VP7 (10).

Four-week-old NOD mice were examined for susceptibility to infection with RRV. All of the mice showed anti-rotavirus antibody titers of <1:50 by EIA immediately prior to RRV inoculation and were housed in microisolator cages in an isolation cabinet of a dedicated quarantine room for the course of the experiment. Groups of 5 female and 5 male mice (10 mice per group) were inoculated orally with 50 μl of RRV (8.0×10^6 fluorescing cell-forming units [FCFU]), a medium dose (37), or 50 μl of a mock-infected control preparation. Of the RRV-inoculated mice, 90% seroconverted to RRV, showing anti-rotavirus antibody titers in sera collected 10 to 16 days after RRV inoculation of ≥1:800 by EIA. Stool samples collected daily for 16 days after RRV inoculation were analyzed for rotavirus antigen by capture EIA as described previously (11), with anti-VP6 mouse monoclonal antibody RVA for detection of bound antigen. Of the RRV-inoculated mice, 70% excreted viral antigen, as detected by EIA, starting at 3 to 7 days after RRV inoculation and continuing for 1 to 7 days. Virus excretion was detected for up to 10 days from the time of RRV inoculation, with 58% of mice showing stationary antigen levels, 14% showing increasing and then decreasing levels, 14% showing decreasing levels, and 14% showing biphasic peaks of excretion at days 5 and 9 after inoculation. Of the female mice that seroconverted to rotavirus, 20% did not excrete viral antigen detectable by EIA. Of the male RRV-inoculated mice, 20% showed a titer of <1:50 by EIA in sera collected 16 days after inoculation, did not excrete RRV detectable by EIA, and thus did not appear to have become infected with RRV. Overall, 90% of RRV-inoculated NOD mice showed evidence of rotavirus infection, which did not appear to be sex dependent. The mock-inoculated mice neither seroconverted to rotavirus nor excreted detectable rotavirus antigen in their stool. No evidence of diarrhea (liquid stool after gentle abdominal palpation, soiling of bedding or fur) or diabetes (frequent urination) was detected during daily examination of mice. The blood glucose levels of these mice were not measured. Overall, RRV infection in adult NOD mice showed patterns of seroconversion, virus shedding, and lack of

symptoms similar to those of other mouse strains, such as BALB/c and CD2 (30, 37).

Monkey, but not human, rotaviruses replicate to a high titer in NOD mouse islets. Islets and islet cell-depleted pancreatic cells from NOD and NOR mice were tested for susceptibility to infection with RRV, SA11, and the prototype human rotavirus strain Wa. Pancreatic islets were isolated from 8-week-old male NOD and NOR mice (eight per experiment) by a modified collagenase technique as previously described (55). Briefly, immediately after euthanasia by CO_2 narcosis, pancreatic ducts of mice were injected with 3.9 U of collagenase P (Boehringer, Mannheim, Germany) in 3.0 ml of DMEM. Pancreata were collected onto ice and incubated at 37°C for 20 min in 10 ml of warm DMEM. Collagenase digestion was stopped by replacement of medium with 10 ml of cold DMEM, and cell clumps were disrupted by shaking for 1 min. Cells were filtered through 500-μm mesh into DMEM and then sedimented twice under gravity for 5 min on ice. The supernatant, containing pancreatic cells depleted of islets, was collected into DMEM supplemented with 2% (vol/vol) fetal calf serum (FCS) (islet cell-depleted pancreatic cells). Sedimented islets were centrifuged at 200 × *g* for 1 min at 4°C, resuspended in 10 ml of Histopaque 1077 (Sigma), and overlaid with 5 ml of DMEM. Cells were centrifuged at gradually increasing speeds (from 25 × *g* to 800 × *g*) for 4 min and then at 800 × *g* for a further 10 min at 4°C. Islets were recovered from the interface, washed twice at 1 × *g* for 1 min with DMEM, hand picked individually into DMEM on ice with a siliconized Pasteur pipette, and counted under a dissecting microscope. As assessed by microscopic examination, the islet purity was 70%.

Freshly isolated, free-floating murine islets (~500; ~5×10^5 cells) in DMEM were infected with trypsin-activated virus at a multiplicity of infection (MOI) of 0.1, 1, or 10 or with trypsin-activated, uninfected MA104 cell lysate for 1 h at 37°C. After virus adsorption, islets were washed twice in DMEM by centrifugation at 1,500 × *g* for 7 min. After the final wash, cells were gently resuspended in DMEM-T and transferred in 100-μl aliquots to wells of 96-well cell culture trays (Nunclon). At 24 to 120 h p.i., cells were collected onto glass slides by cytospin centrifugation at 450 × *g* for 8 min and then fixed in a 3:1 solution of acetone-methanol for 20 min at −20°C.

Freshly isolated, murine islet cell-depleted pancreatic cells were centrifuged at 1,000 × *g*, resuspended in DMEM supplemented with 2% (vol/vol) FCS to 5×10^5 cells/ml, and then infected with trypsin-activated virus or uninfected MA104 cell lysate as for islet cells. After virus adsorption, cells were washed twice in DMEM by centrifugation at 1,000 × *g* for 7 min and maintained in DMEM-T in 100-μl aliquots in the same way as islets. Cells were collected at 18 h p.i. by cytospin centrifugation at 800 × *g* for 8 min onto glass slides and then fixed the same way as islets.

After drying, each slide of cells was stained with 50 μl of a 1:400 dilution in filtered phosphate-buffered saline (PBS) of rabbit hyperimmune antiserum to SA11 or preimmune rabbit serum as a control (11) for 1 h at 37°C. Slides were washed in filtered PBS for 15 min at room temperature with one change of PBS and then counterstained, at 50 μl per slide, with fluorescein isothiocyanate-conjugated sheep anti-rabbit IgG (Silenus Labs Pty. Ltd., Boronia, Victoria, Australia) diluted 1:100 in filtered PBS for 1 h at 37°C. Slides were then washed as described above and photographed immediately. Photographs were taken with a Leitz Diaplan fluorescence microscope (Wild Leitz Pty. Ltd.) and Kodak Elite Chrome 400 film (Eastman Kodak Company, Rochester, N.Y.).

With this immunochemical staining method, RRV replication was detectable in virus-infected islets at 24 h p.i. and the numbers of infected cells per islet increased up to 72 h p.i., when most of the cells on the islet surface were infected (Fig. 1A and B). At 120 h p.i., islets still showed many infected cells (Fig. 1C). Strongly fluorescing RRV-infected cells often appeared to be rounded or partly detached from the islet surface (Fig. 1B, C, and F). Concomitant with virus replication, islets decreased in size, as shown in Fig. 1D (cf. Fig. 1F). It therefore appears that each round of virus replication in the cells on the islet surface results in progressive loss of the surface cells, reducing the size of the islet. This process may have exposed further susceptible cells to infection. SA11 replication was also evident at 24 h p.i. (Fig. 1G), and additional infected cells were detected at 48 h p.i. (Fig. 1H). In Wa rotavirus-infected islets, one or two specifically fluorescing cells per islet were evident at 24 h p.i. (Fig. 1H) and none were detected after that time. Islet cell-depleted pancreatic cells consisted of single cells and clumps of up to five cells, which were a mixture of at least two nonadherent cell types on the basis of size. As assessed by trypan blue exclusion, these cells lost >80% of their viability after culture for 24 h, even in the presence of 2% (vol/vol) FCS. However, one or two RRV-infected cells were visible at 18 h p.i. in cytospins of cells inoculated with virus at an MOI of 1, whereas no stained cells were visible in mock-infected, islet cell-depleted cells (data not shown).

In order to construct virus growth curves, virus-infected and uninfected islets and islet cell-depleted pancreatic cells were prepared as described above. Confluent monolayers of MA104 cells (5×10^4 cells/well) were washed twice with PBS and infected with trypsin-activated rotavirus at an MOI of 0.1, 1, or 10 (RRV) or 1 or 10 (SA11 and Wa). For all cell types, infection was terminated at 1 to 168 h p.i. by freezing at −70°C. Samples were frozen and thawed twice to release intracellular virus. Viral titers were determined by indirect immunofluorescent staining of MA104 cell monolayers inoculated with serial dilutions of virus samples as previously described (8). Viral titers are expressed as the number of FCFU per milliliter.

The titers of infectious RRV produced during virus growth over 72 h in primary NOD mouse islets were compared with the titers in primary intestinal epithelial cells (enterocytes) obtained from the same mice and with the titers in MA104 cells (Fig. 2). In islets, RRV titers increased slowly and steadily up to 72 h p.i. In contrast, the virus titer obtained after inoculation of the MA104 cell monolayers increased rapidly over the first 24 h and then stabilized at a level about 1 $\log_{10}$ higher than that in islet cultures at 72 h p.i. No RRV growth was detected in the enterocytes, which were obtained as small clumps that did not adhere to the solid phase over the course of the experiment. Mock-infected enterocyte cultures showed rapidly declining viabilities (as assessed by trypan blue exclusion) of 83, 42, 41, and 36% after 1, 2.5, 3.5, and 15 h of culture, respectively. The lack of adherence and loss of cellular viability suggest that, in contrast to islets, freshly isolated enterocytes are unable to survive long enough for detectable RRV growth.

Titers of SA11 and Wa in NOD mouse islets were consistent

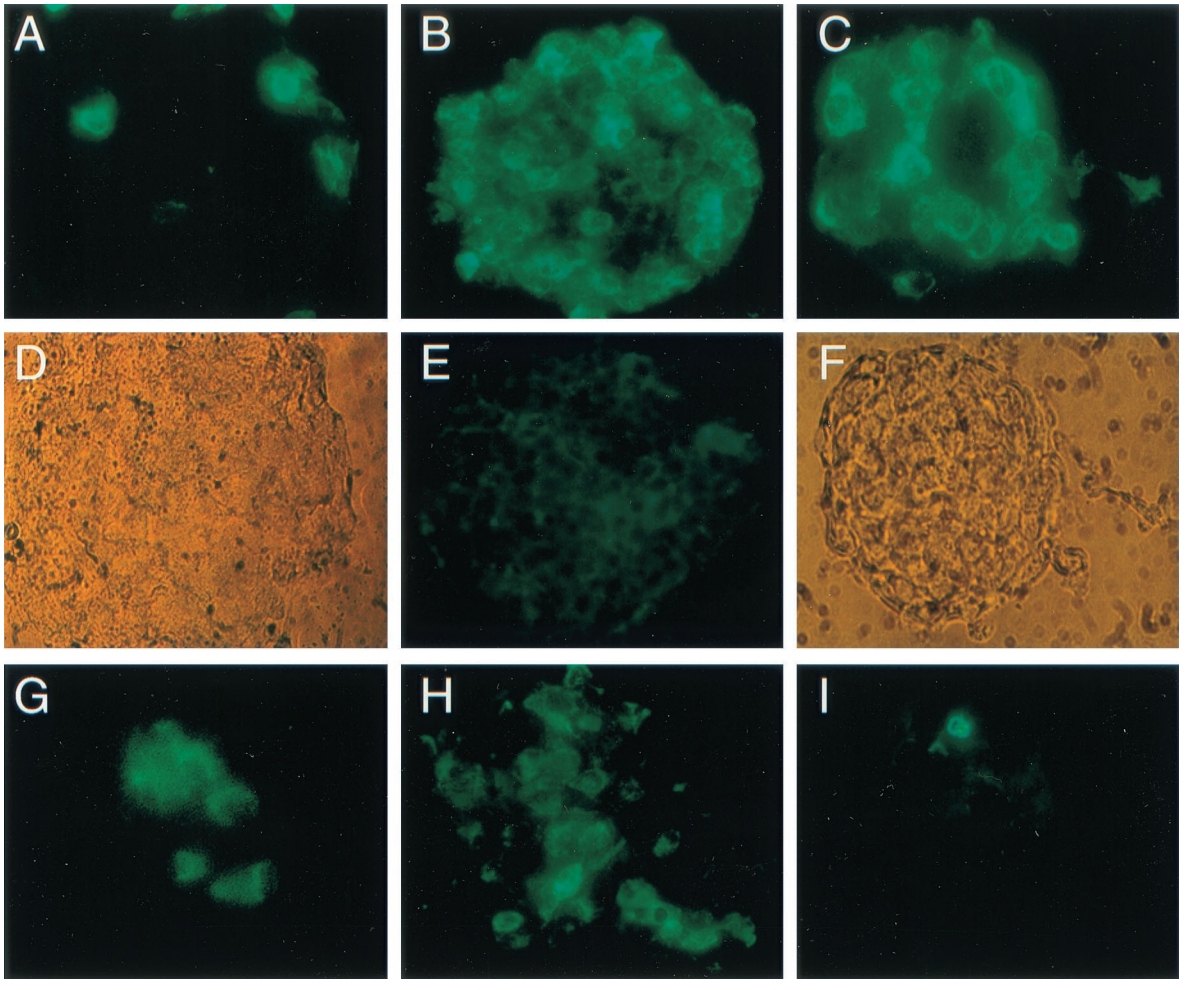

FIG. 1. Detection of RRV, SA11, and Wa antigens in primary NOD mouse islets by indirect immunofluorescence assay after 1 to 5 days of infection at an MOI of 1.0. Rotavirus-infected and uninfected cells were fixed and stained at various times p.i. RRV-infected cells are shown at 24 h (A and D), 72 h (B), and 120 h (C and F) p.i.; uninfected (control) cells are shown at 72 h p.i. (E); SA11-infected cells are shown at 24 h (G) and 48 h (H) p.i.; and Wa-infected cells are shown at 24 h p.i. (I). Infected cells were visualized by fluorescence microscopy (A, B, C, E, G, H, and I). The position of RRV-infected cells within the islet was located by phase-contrast microscopy (D and F). Magnification, ×200.

with the results of immunochemical staining of infected islets. SA11 titers in islet cultures increased gradually to maxima at 168 h p.i. of 1.0×10^6 FCFU/ml at an MOI of 0.1 and 5.2×10^5 FCFU/ml at an MOI of 1 (Fig. 3, Table 1). The maximum titer of SA11 in islets at an MOI of 1 was 130-fold lower than the maximum titer of SA11 in MA104 cells at the same MOI. Very little, if any, replication of Wa rotavirus was detected in islets, as virus titers in islet cultures did not change significantly over 168 h (Table 1). SA11 titers in islet cell-depleted pancreatic cells, at MOIs of 0.1 and 1, did not show any increase over the input virus titer (data not shown). At MOIs of 1 and 10, Wa titers in islet cell-depleted pancreatic cells declined over 168 h, showing no evidence of virus growth (data not shown).

RRV replicates to higher titers in NOD mouse islets than in NOR mouse islets. The kinetics of RRV growth in NOD and NOR mouse islets and islet cell-depleted pancreatic cells over 7 days are compared with those in MA104 cells, at MOIs of 0.1 and 1, in Fig. 4. In islets and MA104 cells, the maximum virus yield was obtained at an MOI of 0.1. As shown in Fig. 4 and Table 1, virus titers in NOD mouse islets rose steadily to

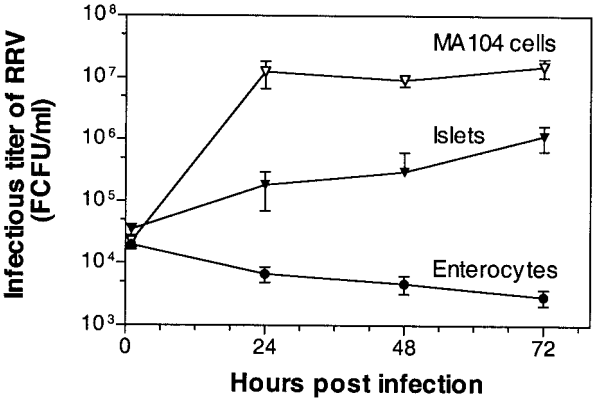

FIG. 2. Relative growth of RRV in primary NOD mouse islets, enterocytes, and MA104 cells up to 72 h p.i. at an MOI of 1.0. Enterocytes were isolated from the same mice from which the pancreatic cells were obtained, as described previously (36), but were infected immediately, without culturing in vitro. Each bar represents the 95% confidence interval of the mean of three replicates.

TABLE 1. Maximum rotavirus titers and maximum increases in virus titers over input produced by monkey and human rotaviruses in cultures of primary islet cells from mice, pigs, and monkeys

Rotavirus strain	MOI	Maximum virus titer in FCFU/ml (fold increase in titer over input[a]) in given islet cell type:			
		Mouse		Pig	Monkey[b]
		NOD	NOR		
RRV[c]	0.1	1.7×10^7 (4,570)	1.9×10^6 (503)	ND[g]	ND
	1	7.0×10^6 (269)	2.6×10^6 (125)	ND	3.9×10^4 (23)
SA11[d]	0.1	1.0×10^6 (1,300)	ND	ND	ND
	0.5–1	5.2×10^5 (140)	ND	8.4×10^4 (40)	1.7×10^4 (20)
	10	1.3×10^5 (4.9)	ND	6.5×10^6 (3,170)	ND
Wa[e]	1	4.2×10^3 (1.2)	ND	ND	6.0×10^3 (6.0)
RV-5[f]	0.5–1	ND	ND	3.8×10^3 (1.0)	4.4×10^3 (3.3)

[a] Input titer is defined as the titer of cell-associated virus at 1 h p.i.
[b] Maximum virus titers of all rotaviruses were reached at 72 h p.i. in monkey islets.
[c] Maximum RRV titers were reached at 120 h p.i. in NOD and NOR mouse islets.
[d] Maximum SA11 titers were reached at 168 h p.i. in NOD mouse islets and at 24 h in pig islet cells.
[e] Maximum Wa titers were reached at 24 h p.i. in NOD mouse islets.
[f] Maximum RV-5 titers were reached at 24 h p.i. in pig islet cells.
[g] ND, not done.

maxima at 120 h p.i., which were five- to sevenfold lower than the maximum titers in MA104 cells at the same MOI. NOR mouse islets were less susceptible to RRV infection than were islets from NOD mice (Fig. 4; Table 1). This effect was greater at an RRV MOI of 0.1 (Fig. 4A) but was also evident at an MOI of 1 (Fig. 4B). RRV titers in NOR and NOD mouse islets were similar at 168 h p.i., but titers at 24 to 120 h p.i. were always lower in NOR mice than in NOD mice. The maximum difference in titer between NOR and NOD mouse islets was at 72 h p.i. at an MOI of 0.1, when NOR islets showed 320-fold lower titers than NOD islets (Fig. 4A). Maximum titers in MA104 cells were reached at 72 h p.i. (MOI, 0.1; Fig. 4A) and 24 h p.i. (MOI, 1; Fig. 4B). The slower rate of RRV growth in NOD and NOR mouse islets than in MA104 cells may result from the restricted access of virus to susceptible cells imposed by the spherical nature of islets. In contrast to islets, almost all of the cells in the MA104 cell monolayer would be accessible to virus at the time of inoculation.

At an MOI of 0.1, the RRV titer in islet cell-depleted pancreatic cells increased 9.8-fold over the input, to a maximum of 2.5×10^4 FCFU/ml at 120 h p.i. (Fig. 4A). At an MOI of 1, the maximum RRV titer of 1.3×10^6 FCFU/ml was reached at 96 h p.i., which was a 209-fold increase over the input (Fig. 4B). In order for RRV titers in MA104 cells to be comparable to those in the islet cell-depleted pancreatic cells, MA104 cells also were inoculated with RRV in the presence of 2% (vol/vol) FCS, which reduced the maximum RRV titer by 2.2-fold at an MOI of 1 (data not shown). The maximum RRV titer in islet cell-depleted pancreatic cells at an MOI of 1 was 30-fold lower than that in MA104 cells grown in the presence of FCS. At MOIs of 10 and 100, RRV titers in islet cell-depleted pancreatic cells increased 2.0- and 1.2-fold, respectively (data not shown).

Monkey, but not human, rotaviruses replicate in porcine islets. To obtain cultured fetal porcine proislet cells, pancreatic fragments from late-gestation outbred Landrace fetal pigs were incubated with collagenase (type XI; Sigma) (21) and cultured in 95% O_2–5% CO_2 at 37°C for 3 days to reduce the amount of nonendocrine tissue. After 2 days of further culture in 90% air–10% CO_2, proislet cells were harvested by hand picking (21) and single cells were prepared by digestion at 37°C in 0.1% (wt/vol) porcine trypsin for 45 min, followed by 87 mg of collagenase (type XI; Sigma) per ml for 7 min. Cells were washed twice in DMEM by centrifugation at 1,000 × *g* for 6 min and allowed to recover in culture overnight at 37°C in DMEM-F10. Cells were centrifuged at 1,000 × *g*, resuspended in DMEM to 8×10^5 cells/ml, infected with trypsin-activated SA11, RV5, or P rotavirus or uninfected MA104 cell lysate, and then washed and resuspended in DMEM-T in the same way as murine islets were. Cells were transferred to 24-well cell culture plates (Nunclon). Infection was terminated, and the virus titer was determined as it was in MA104 cells. Over 24 h, fetal porcine proislets supported more than 3 $\log_{10}$ of SA11 growth at an MOI of 10 and almost 2 $\log_{10}$ of SA11 growth at

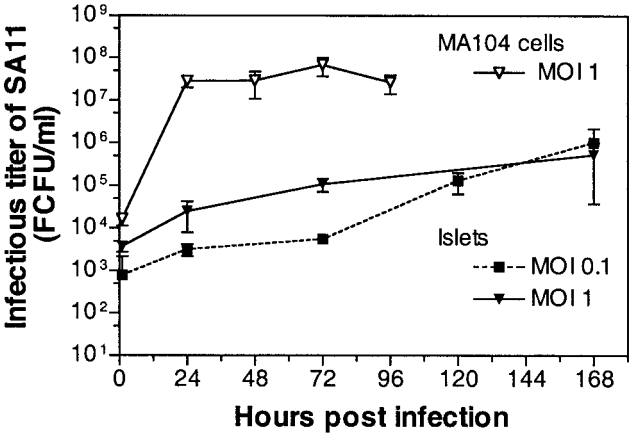

FIG. 3. Kinetics of SA11 growth over 7 days in primary NOD mouse islets at MOIs of 0.1 and 1. The growth curve of SA11 in MA104 cells at an MOI of 1 is included for comparison. Each bar represents the 95% confidence interval of the mean of replicates in two experiments.

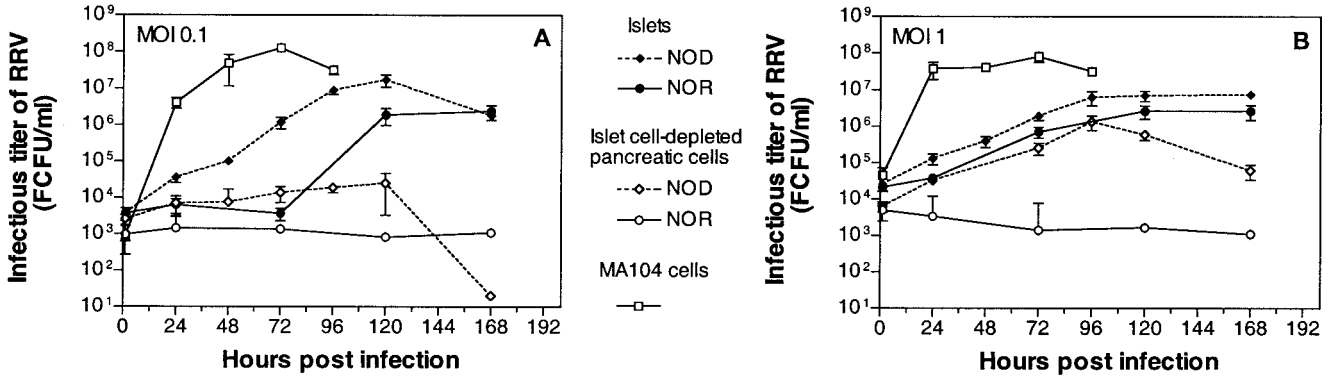

FIG. 4. Kinetics of RRV growth over 7 days in primary NOD and NOR mouse islets and islet cell-depleted pancreatic cells at MOIs of 0.1 (A) and 1 (B). Growth curves of RRV at the same MOI in MA104 cells are included for comparison. Each bar represents the 95% confidence interval of the mean of replicates obtained in two to four experiments.

an MOI of 0.5. As shown in Table 1, at an MOI of 10, SA11 titers increased from a mean ± a standard deviation of $2.1 \times 10^3 \pm 3.9 \times 10^2$ FCFU/ml at 1 h p.i. to $6.5 \times 10^6 \pm 9.4 \times 10^5$ FCFU/ml at 24 h p.i. In contrast, low and stationary or low and decreasing titers of rotaviruses P (MOI, 0.5, 10) and RV-5 (MOI, 0.5) were detected to 24 h p.i., showing that little or no replication of these rotaviruses occurred.

Human and monkey rotaviruses replicate in monkey islets. The ability of rotaviruses to replicate in monkey islets, prepared similarly to human islets (6), was examined. Pancreata were obtained from two adult female pigtailed macaques (*Macaca nemestrina*) housed in the Australian National Macaque Facility that were being culled because of age. Excised pancreata were transported in ice-cold Ross' perfusion solution for 1 h. Pancreata, minced into 2-mm^3 blocks, were incubated at 37°C with agitation at 400 rpm on a horizontal rotator (Infors AG) in RPMI 1640 medium containing 3 mg of collagenase P (Roche Diagnostic GmbH, Mannheim, Germany) per ml. The supernatant was collected after 40 min and diluted in ice-cold RPMI 1640 medium containing 10% (vol/vol) FCS (RPMI-FCS). This process was repeated once on the remaining pieces of pancreas. Resultant cells were gently washed twice in RPMI-FCS by centrifugation at 500×g, and islets were hand picked into RPMI-FCS. Islet purity, as determined by microscopic examination, was 60%. Islets were infected with the Wa, RV-5, RRV, and SA11 rotaviruses at an MOI of 1 as described above. As shown in Fig. 5 and Table 1, all of the rotavirus strains tested replicated in the monkey islets and reached maximum titers at 72 h p.i.

Relative growth of rotaviruses in islets of different species. In monkey islets, strain Wa titers increased 6.0-fold over the input whereas in NOD mouse islets, strain Wa titers were stationary (Table 1; Fig. 5A). Strain RV-5 titers in monkey islets increased 3.3-fold over the input but were unchanged in porcine islets (Table 1; Fig. 5B). Overall, the human rotaviruses grew only in monkey islets and to lower titers than did monkey strains. This is consistent with previous studies showing that cell lines permissive to infection with these human rotaviruses are restricted to monkey kidney (MA104) and human colonic adenocarcinoma types (34). Surprisingly, as shown in Table 1, stains RRV and SA11 grew to the highest titers in heterologous murine islets and to the lowest titers in homolo-

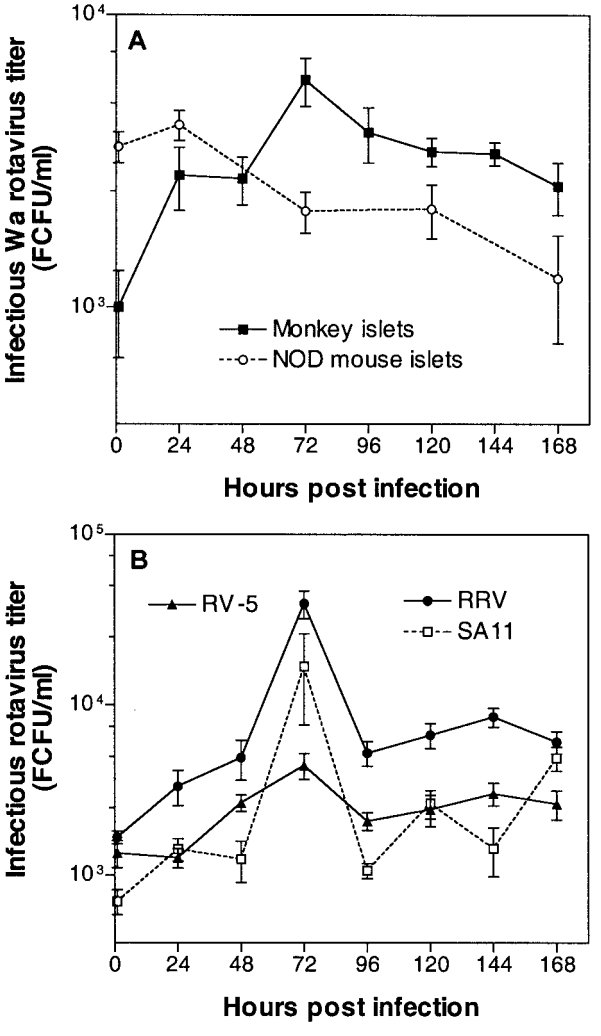

FIG. 5. Kinetics of growth of human and monkey rotaviruses at an MOI of 1 in primary adult monkey islets. Strain Wa replication in monkey islets is compared with titers of strain Wa in primary NOD mouse islets (A). Growth curves of rotavirus strains RV-5, RRV, and SA11 in primary adult monkey islets are shown in panel B. Each bar represents the standard deviation of the mean of three replicates from each of two experiments.

gous monkey islets. Possibly, the monkey islets were more resistant to infection because of the age of the monkeys or differences in the protocols required to produce purified islets. The monkey islets contained a distinct outer margin containing a single layer of columnar cells that was absent from the porcine and murine islets. This layer may have rendered the monkey islets more resistant to infection.

At an MOI of 10, strain SA11 replicated to a higher titer in porcine proislets than in murine islets (Table 1). The differences in the virus titers produced suggest that at a high MOI, the porcine proislets were more susceptible to strain SA11 rotavirus infection than were the NOD mouse islets, but at a low MOI, the reverse applied. Maximum SA11 titers were reached much more slowly in NOD mouse islets (7 days p.i.) than in porcine proislets (24 h p.i.). The maintenance of the porcine proislets as individual cells in culture is likely to have led to selection of less well-differentiated cells (58) that may have been more susceptible to infection. Also, as the structure of the porcine islet was disrupted prior to culture, virions may have accessed cells and receptors not available on the surface of the murine islet.

The present study shows that whereas culture-adapted primate rotavirus strains RRV and SA11 are able to infect and replicate to high titers in primary pancreatic cells, particularly islet cells, from mice, pigs, and monkeys, human rotavirus growth is detectable only in monkey islets. Islets from adult, diabetes-prone NOD mice were highly susceptible to infection with RRV, whereas those from control, non-diabetes-prone NOR mice were less susceptible. Most of the cells on the islet appeared to be infected with RRV and produced large amounts of viral antigen. Multiple cycles of RRV infection were evident in islets, with each cycle apparently leading to loss of adhesion of infected cells and exposure of a new layer of cells within the islet, which subsequently was also infected. These islet cultures produced maximum levels of infectious RRV at 5 days p.i. that were only 14% lower than the maximum titers produced in the highly permissive MA104 cells. Islets of 8-week-old NOD mice comprise ≥80% insulin-producing β cells, with glucagon- and somatostatin-producing cells being located mainly at the islet edge (3). The majority of NOD mouse islet cells were infected with RRV, so the infected cells would have been predominantly β cells.

NOD mouse islets were from 8-week-old mice with insulitis. T cells in the insulitis lesion are integrin α4β7 high (19), as are GAD-reactive T cells in humans with recently diagnosed T1D (43). Lymphocyte homing to the intestine and to the pancreas is mediated by binding of α4β7 to mucosal addressin cell adhesion molecule 1, which is expressed on intestinal and peri-islet-high endothelial venules. The major difference between NOD and NOR islets is the presence of inflammation, consisting of α4β7-high T cells, in the NOD islets (19). In the light of the decreased growth of rotaviruses in NOR islets over NOD islets, it is of interest that rotavirus VP4 and VP7 contain sequences that can be recognized by both α4β1 and α4β7 (9, 23, 34) and that SA11 has been shown to bind to cell surface α4β1 integrin, leading to productive infection (23).

Primary enterocytes harvested from NOD mice did not support RRV infection and rapidly lost viability. It has been shown that less than 5% of the enterocytes harvested from BALB/c mice by this method become adherent and generate colonies of new cells and that the latter cells do support a 37-fold increase in RRV titer at 1 day p.i. at an MOI of 10 (36). In contrast to enterocytes, primary islets were susceptible to RRV and other rotaviruses without recourse to culture.

Consistent with the detection in murine islets of fewer SA11 virus-infected cells than RRV-infected cells at 1 and 3 days p.i., the maximum SA11 titers produced in these islets were 13- to 17-fold lower than those obtained with RRV at the same MOI. Evidence of growth of RRV and SA11 in NOD mouse islet cell-depleted pancreatic cells was obtained. However, it is not completely clear to what extent these non-islet pancreatic cells are able to support RRV and SA11 infection. The cell preparations used were those remaining after islet purification and may have contained residual islet cells. Islet cell-depleted pancreatic cells also routinely show reduced viabilities compared with islets because of release of proteases from the exocrine cells (38), which also may have affected the virus titers produced.

This demonstration that RRV, Wa, RV-5, and SA11 are able to infect islets shows that rotavirus infection of the pancreas could be possible in vivo in an animal model (by analogy with reovirus) and in humans. These findings lend support to our previous studies implicating rotavirus as a trigger for islet autoimmunity in children. Should direct infection of the pancreas leading to islet autoimmunity occur in vivo, it would not necessarily be to the exclusion of molecular mimicry between T-cell epitopes on rotavirus VP7 and IA-2 or GAD. It is likely that both direct infection and molecular mimicry could operate synergistically to promote ongoing islet autoimmunity.

B.S.C. and M.C.H. contributed equally to this work.

We are grateful to Stephen Kent and Russell Mitton for advice and assistance in the provision of monkey pancreas, to Maria Koulmanda for technical assistance, and to Kate Graham for help with preparation of the manuscript.

This work was supported by the Juvenile Diabetes Research Foundation International. B.S.C. is a Senior Research Fellow and L.C.H. is a Senior Principal Research Fellow of the National Health and Medical Research Council of Australia.

REFERENCES

1. **Atkinson, M. A., and E. H. Leiter.** 1999. The NOD mouse model of type 1 diabetes: as good as it gets? Nat. Med. **5:**601–604.
2. **Bingley, P. J., E. Bonifacio, A. J. Williams, S. Genovese, G. F. Bottazzo, and E. A. Gale.** 1997. Prediction of IDDM in the general population: strategies based on combinations of autoantibody markers. Diabetes **46:**1701–1710.
3. **Bishop, A. E., and J. M. Polak.** 1991. The anatomy, organization and ultrastructure of the islets of Langerhans, p. 57–71. *In* G. Williams (ed.), Textbook of diabetes, vol. I. Blackwell, Oxford, United Kingdom.
4. **Bishop, R. F., L. E. Unicomb, and G. L. Barnes.** 1991. Epidemiology of rotavirus serotypes in Melbourne, Australia, from 1973 to 1989. J. Clin. Microbiol. **29:**862–868.
5. **Buesa, J., J. V. Raga, J. Colomina, C. O. de Souza, C. Munoz, and M. T. Gil.** 1999. Rotavirus-specific cytotoxic T lymphocytes recognize overlapping epitopes in the amino-terminal region of the VP7 glycoprotein. Virology **257:**424–437.
6. **Campbell, I. L., P. G. Colman, and L. C. Harrison.** 1985. Adult human pancreatic islet cells in tissue culture: function and immunoreactivity. J. Clin. Endocrinol. Metab. **61:**681–685.
7. **Campbell, I. L., L. C. Harrison, R. G. Ashcroft, and I. Jack.** 1988. Reovirus infection enhances expression of class I MHC proteins on human beta-cell and rat RINm5F cell. Diabetes **37:**362–365.
8. **Coulson, B. S., K. J. Fowler, R. F. Bishop, and R. G. Cotton.** 1985. Neutralizing monoclonal antibodies to human rotavirus and indications of antigenic drift among strains from neonates. J. Virol. **54:**14–20.
9. **Coulson, B. S., S. L. Londrigan, and D. J. Lee.** 1997. Rotavirus contains integrin ligand sequences and a disintegrin-like domain that are implicated in virus entry into cells. Proc. Natl. Acad. Sci. USA **94:**5389–5394.
10. **Coulson, B. S., J. M. Tursi, W. J. McAdam, and R. F. Bishop.** 1986. Deri-

vation of neutralizing monoclonal antibodies to human rotaviruses and evidence that an immunodominant neutralization site is shared between serotypes 1 and 3. Virology **154:**302–312.
11. **Coulson, B. S., L. E. Unicomb, G. A. Pitson, and R. F. Bishop.** 1987. Simple and specific enzyme immunoassay using monoclonal antibodies for serotyping human rotaviruses. J. Clin. Microbiol. **25:**509–515.
12. **De La Rubia, L., M. I. Herrera, M. Cebrero, and J. C. De Jong.** 1996. Acute pancreatitis associated with rotavirus infection. Pancreas **12:**98–99.
13. **Estes, M. K.** 2001. Rotaviruses and their replication, p. 1747–1785. *In* P. M. Howley (ed.), Fields virology, 4th ed., vol. 2. Lippincott, Williams & Wilkins, Philadelphia, Pa.
14. **Fox, C. J., and J. S. Danska.** 1998. Independent genetic regulation of T-cell and antigen-presenting cell participation in autoimmune islet inflammation. Diabetes **47:**331–338.
15. **Franco, M. A., I. Prieto, M. Labbe, D. Poncet, F. Borras-Cuesta, and J. Cohen.** 1993. An immunodominant cytotoxic T cell epitope on the VP7 rotavirus protein overlaps the H2 signal peptide. J. Gen. Virol. **74:**2579–2586.
16. **Gilger, M. A., D. O. Matson, M. E. Conner, H. M. Rosenblatt, M. J. Finegold, and M. K. Estes.** 1992. Extraintestinal rotavirus infections in children with immunodeficiency. J. Pediatr. **120:**912–917.
17. **Grimwood, K., J. C. Coakley, I. L. Hudson, R. F. Bishop, and G. L. Barnes.** 1988. Serum aspartate aminotransferase levels after rotavirus gastroenteritis. J. Pediatr. **112:**597–600.
18. **Grunow, J. E., S. F. Dunton, and J. L. Waner.** 1985. Human rotavirus-like particles in a hepatic abscess. J. Pediatr. **106:**73–76.
19. **Hanninen, A., C. Taylor, P. R. Streeter, L. S. Stark, J. M. Sarte, J. A. Shizuru, O. Simell, and S. A. Michie.** 1993. Vascular addressins are induced on islet vessels during insulitis in nonobese diabetic mice and are involved in lymphoid cell binding to islet endothelium. J. Clin. Investig. **92:**2509–2515.
20. **Harrison, L. C.** 2001. Risk assessment, prediction and prevention of type 1 diabetes. Pediatr. Diabetes **2:**71–82.
21. **Harrison, L. C., S. X. Chu, H. J. DeAizpurua, M. Graham, M. C. Honeyman, and P. G. Colman.** 1992. Islet-reactive T cells are a marker of preclinical insulin-dependent diabetes. J. Clin. Investig. **89:**1161–1165.
22. **Hayashi, T., H. Iwata, and T. Onodera.** 1999. Role of interleukin-2 in pancreatic islet-cell destruction in reovirus type 2-infected DBA/1 suckling mice. J. Comp. Pathol. **120:**313–320.
23. **Hewish, M. J., Y. Takada, and B. S. Coulson.** 2000. Integrins $\alpha 2\beta 1$ and $\alpha 4\beta 1$ can mediate SA11 rotavirus attachment and entry into cells. J. Virol. **74:**228–236.
24. **Honeyman, M. C., B. S. Coulson, and L. C. Harrison.** 2000. A novel subtype of type 1 diabetes mellitus. N. Engl. J. Med. **342:**1835.
25. **Honeyman, M. C., B. S. Coulson, N. L. Stone, S. A. Gellert, P. N. Goldwater, C. E. Steele, J. J. Couper, B. D. Tait, P. G. Colman, and L. C. Harrison.** 2000. Association between rotavirus infection and pancreatic islet autoimmunity in children at risk of developing type 1 diabetes. Diabetes **49:**1319–1324.
26. **Honeyman, M. C., N. L. Stone, and L. C. Harrison.** 1998. T-cell epitopes in type 1 diabetes autoantigen tyrosine phosphatase IA-2: potential for mimicry with rotavirus and other environmental agents. Mol. Med. **4:**231–239.
27. **Horwitz, M. S., L. M. Bradley, J. Harbertson, T. Krahl, J. Lee, and N. Sarvetnick.** 1998. Diabetes induced by Coxsackie virus: initiation by bystander damage and not molecular mimicry. Nat. Med. **4:**781–785.
28. **Hoshino, Y., L. J. Saif, S. Y. Kang, M. M. Sereno, W. K. Chen, and A. Z. Kapikian.** 1995. Identification of group A rotavirus genes associated with virulence of a porcine rotavirus and host range restriction of a human rotavirus in the gnotobiotic piglet model. Virology **209:**274–280.
29. **Jun, H. S., and J. W. Yoon.** 2001. The role of viruses in type I diabetes: two distinct cellular and molecular pathogenic mechanisms of virus-induced diabetes in animals. Diabetologia **44:**271–285.
30. **Khoury, C. A., K. A. Brown, J. E. Kim, and P. A. Offit.** 1994. Rotavirus-specific intestinal immune response in mice assessed by enzyme-linked immunospot assay and intestinal fragment culture. Clin. Diagn. Lab. Immunol. **1:**722–728.
31. **Kirkwood, C. D., R. F. Bishop, and B. S. Coulson.** 1998. Attachment and growth of human rotaviruses RV-3 and S12/85 in Caco-2 cells depend on VP4. J. Virol. **72:**9348–9352.
32. **Kitamoto, N., R. F. Ramig, D. O. Matson, and M. K. Estes.** 1991. Comparative growth of different rotavirus strains in differentiated cells (MA104, HepG2, and CaCo-2). Virology **184:**729–737.
33. **Koulmanda, M., J. Kovarik, and T. E. Mandel.** 1998. Cyclophosphamide, but not CTLA4Ig, prolongs survival of fetal pig islet grafts in anti-T cell monoclonal antibody-treated NOD mice. Xenotransplantation **5:**215–221.
34. **Londrigan, S. L., M. J. Hewish, M. J. Thomson, G. M. Sanders, H. Mustafa, and B. S. Coulson.** 2000. Growth of rotaviruses in continuous human and monkey cell lines that vary in their expression of integrins. J. Gen. Virol. **81:**2203–2213.
35. **Ludert, J. E., N. Feng, J. H. Yu, R. L. Broome, Y. Hoshino, and H. B. Greenberg.** 1996. Genetic mapping indicates that VP4 is the rotavirus cell attachment protein in vitro and in vivo. J. Virol. **70:**487–493.
36. **Macartney, K. K., D. C. Baumgart, S. R. Carding, J. O. Brubaker, and P. A. Offit.** 2000. Primary murine small intestinal epithelial cells, maintained in long-term culture, are susceptible to rotavirus infection. J. Virol. **74:**5597–5603.
37. **Moser, C. A., S. Cookinham, S. E. Coffin, H. F. Clark, and P. A. Offit.** 1998. Relative importance of rotavirus-specific effector and memory B cells in protection against challenge. J. Virol. **72:**1108–1114.
38. **Nevalainen, T. J., and J. Anttinen.** 1977. Ultrastructural and functional changes in pancreatic acinar cells during autolysis. Virchows Arch. B Cell Pathol. **24:**197–207.
39. **Nigro, G.** 1991. Pancreatitis with hypoglycemia-associated convulsions following rotavirus gastroenteritis. J. Pediatr. Gastroenterol. Nutr. **12:**280–282.
40. **Offit, P. A., G. Blavat, H. B. Greenberg, and H. F. Clark.** 1986. Molecular basis of rotavirus virulence: role of gene segment 4. J. Virol. **57:**46–49.
41. **Onodera, T., A. B. Jenson, J. W. Yoon, and A. L. Notkins.** 1978. Virus-induced diabetes mellitus: reovirus infection of pancreatic beta cells in mice. Science **201:**529–531.
42. **Onodera, T., A. Toniolo, U. R. Ray, A. B. Jenson, R. A. Knazek, and A. L. Notkins.** 1981. Virus-induced diabetes mellitus. XX. Polyendocrinopathy and autoimmunity. J. Exp. Med. **153:**1457–1473.
43. **Paronen, J., P. Klemetti, J. M. Kantele, E. Savilahti, J. Perheentupa, H. K. Akerblom, and O. Vaarala.** 1997. Glutamate decarboxylase-reactive peripheral blood lymphocytes from patients with IDDM express gut-specific homing receptor $\alpha 4\beta 7$-integrin. Diabetes **46:**583–588.
44. **Petersen, C., M. Kuske, E. Bruns, D. Biermanns, P. V. Wussow, and H. Mildenberger.** 1998. Progress in developing animal models for biliary atresia. Eur. J. Pediatr. Surg. **8:**137–141.
45. **Prasad, B. V., J. W. Burns, E. Marietta, M. K. Estes, and W. Chiu.** 1990. Localization of VP4 neutralization sites in rotavirus by three-dimensional cryo-electron microscopy. Nature **343:**476–479.
46. **Prochazka, M., D. V. Serreze, W. N. Frankel, and E. H. Leiter.** 1992. NOR/Lt mice: MHC-matched diabetes-resistant control strain for NOD mice. Diabetes **41:**98–106.
47. **Roivainen, M., P. Ylipaasto, J. Ustinov, T. Hovi, and T. Otonkoski.** 2001. Screening enteroviruses for beta-cell tropism using foetal porcine beta-cells. J. Gen. Virol. **82:**1909–1916.
48. **Rother, K. I., and W. F. Schwenk II.** 1995. An unusual case of the nonketotic hyperglycemic syndrome during childhood. Mayo Clin. Proc. **70:**62–65.
49. **Sadeharju, K., M. Lonnrot, T. Kimpimaki, K. Savola, S. Erkkila, T. Kalliokoski, P. Savolainen, P. Koskela, J. Ilonen, O. Simell, M. Knip, and H. Hyoty.** 2001. Enterovirus antibody levels during the first two years of life in prediabetic autoantibody-positive children. Diabetologia **44:**818–823.
50. **Sato, K., Y. Inaba, T. Shinozaki, R. Fujii, and M. Matumoto.** 1981. Isolation of human rotavirus in cell cultures: brief report. Arch. Virol. **69:**155–160.
51. **Saulsbury, F. T., J. A. Winkelstein, and R. H. Yolken.** 1980. Chronic rotavirus infection in immunodeficiency. J. Pediatr. **97:**61–65.
52. **Schwarz, K. B., T. J. Moore, R. E. Willoughby, Jr., S. B. Wee, S. L. Vonderfecht, and R. H. Yolken.** 1990. Growth of group A rotaviruses in a human liver cell line. Hepatology **12:**638–643.
53. **Soike, K. F., G. W. Gary, and S. Gibson.** 1980. Susceptibility of nonhuman primate species to infection by simian rotavirus SA-11. Am. J. Vet. Res. **41:**1098–1103.
54. **Theil, K. W., E. H. Bohl, R. F. Cross, E. M. Kohler, and A. G. Agnes.** 1978. Pathogenesis of porcine rotaviral infection in experimentally inoculated gnotobiotic pigs. Am. J. Vet. Res. **39:**213–220.
55. **Thomas, H. E., J. L. Parker, R. D. Schreiber, and T. W. Kay.** 1998. IFN-gamma action on pancreatic beta cells causes class I MHC upregulation but not diabetes. J. Clin. Investig. **102:**1249–1257.
56. **Tyler, K. L., R. J. Sokol, S. M. Oberhaus, M. Le, F. M. Karrer, M. R. Narkewicz, R. W. Tyson, J. R. Murphy, R. Low, and W. R. Brown.** 1998. Detection of reovirus RNA in hepatobiliary tissues from patients with extrahepatic biliary atresia and choledochal cysts. Hepatology **27:**1475–1482.
57. **Uhnoo, I., M. Riepenhoff-Talty, T. Dharakul, P. Chegas, J. E. Fisher, H. B. Greenberg, and P. L. Ogra.** 1990. Extramucosal spread and development of hepatitis in immunodeficient and normal mice infected with rhesus rotavirus. J. Virol. **64:**361–368.
58. **Wang, R. N., and L. Rosenberg.** 1999. Maintenance of beta-cell function and survival following islet isolation requires reestablishment of the islet-matrix relationship. J. Endocrinol. **163:**181–190.